ISSN 1674-1056
http://cpb.iphy.ac.cn
http://iopscience.iop.org/cpb
中国物理 B
Chinese Physics
中国物理
Chinese Physics B

Improvement of radiative recombination rate in deep ultraviolet laser diodes with step-like quantum barrier and aluminum-content graded electron blocking layer

Yi-Fu Wang(王一夫)[1,2,3], Mussaab I Niass[1,2,3], Fang Wang(王芳)[1,2,3], Yu-Huai Liu(刘玉怀)[1,2,3]

Citation: Chin. Phys. B . 2020, 29(1): 017301 . **doi:** 10.1088/1674-1056/ab592c
Journal homepage: http://cpb.iphy.ac.cn; http://iopscience.iop.org/cpb

What follows is a list of articles you may be interested in

Optical response of an inverted InAs/GaSb quantum well in an in-plane magnetic field

Xiaoguang Wu(吴晓光)

Chin. Phys. B . 2019, 28(10): 107302 . **doi:** 10.1088/1674-1056/ab3c29

Raman spectrum study of δ-doped GaAs/AlAs multiple-quantum wells

Wei-Min Zheng(郑卫民), Wei-Yan Cong(丛伟艳), Su-Mei Li(李素梅), Ai-Fang Wang(王爱芳), Bin Li(李斌), Hai-Bei Huang(黄海北)

Chin. Phys. B . 2018, 27(1): 017302 . **doi:** 10.1088/1674-1056/27/1/017302

Excitonic transitions in Be-doped GaAs/AlAs multiple quantum well

Wei-Min Zheng(郑卫民), Su-Mei Li(李素梅), Wei-Yan Cong(丛伟艳), Ai-Fang Wang(王爱芳), Bin Li(李斌), Hai-Bei Huang(黄海北)

Chin. Phys. B . 2016, 25(4): 047302 . **doi:** 10.1088/1674-1056/25/4/047302

Landau level transitions in InAs/AlSb/GaSb quantum wells

Wu Xiao-Guang, Pang Mi

Chin. Phys. B . 2015, 24(9): 097301 . **doi:** 10.1088/1674-1056/24/9/097301

Intersubband transitions in $In_xAl_{(1-x)}N/In_yGa_{(1-y)}N$quantum well operating at 1.55 μm

Hassen Dakhlaoui

Chin. Phys. B . 2014, 23(9): 097304 . **doi:** 10.1088/1674-1056/23/9/097304

Improvement of radiative recombination rate in deep ultraviolet laser diodes with step-like quantum barrier and aluminum-content graded electron blocking layer*

Yi-Fu Wang(王一夫)[1,2,3], Mussaab I Niass[1,2,3], Fang Wang(王芳)[1,2,3,†], and Yu-Huai Liu(刘玉怀)[1,2,3,‡]

[1] *National Center of International Joint Research for Electronic Materials and Systems, Zhengzhou University, Zhengzhou* 450001, *China*
[2] *International Joint Laboratory of Electronic Materials and Systems, Zhengzhou University, Zhengzhou* 450001, *China*
[3] *School of Information Engineering, Zhengzhou University, Zhengzhou* 450001, *China*

(Received 12 June 2019; revised manuscript received 15 October 2019; accepted manuscript online 20 November 2019)

The design of the active region structures, including the modifications of structures of the quantum barrier (QB) and electron blocking layer (EBL), in the deep ultraviolet (DUV) AlGaN laser diode (LD) is investigated numerically with the Crosslight software. The analyses focus on electron and hole injection efficiency, electron leakage, hole diffusion, and radiative recombination rate. Compared with the reference QB structure, the step-like QB structure provides high radiative recombination and maximum output power. Subsequently, a comparative study is conducted on the performance characteristics with four different EBLs. For the EBL with different Al mole fraction layers, the higher Al-content AlGaN EBL layer is located closely to the active region, leading the electron current leakage to lower, the carrier injection efficiency to increase, and the radiative recombination rate to improve.

Keywords: radiative recombination rate, step-like quantum barrier, aluminum-content-graded EBL

PACS: 73.21.Fg, 73.61.Ey, 78.60.Fi **DOI:** 10.1088/1674-1056/ab592c

1. Introduction

Deep ultraviolet (DUV) laser diodes (LDs) can possess a variety of applications related to chemical analysis, medical and biological reagent detection, diagnostic equipment, high-density data storage, water purification, and material processing.[1–4] Semiconductors containing nitrogen and trivalent elements (such as GaN, InGaN, and AlGaN) are very important for modern optoelectronic applications, including being used as LD active materials and light sources. These nitrides typically possess a high energy bandgap and consequently by very high electron density and hole density as well as relatively low mobility of these particles.[5] Compared with other widely used DUV sources, AlGaN-based DUV LDs are compact, long-lasting, and environmentally-friendly. For III-nitride LDs, the electron has much higher mobility than the hole, whereby it tends to flow over the active region into the p-type layers.[6] These overflown electrons do not contribute to the radiative recombination occurring in the active region. Thus, they are underutilized. Additionally, these electrons can recombine with the holes in the p-type regions, which will reduce the hole injection efficiency.[7,8] Such an electron overflow and a low radiative recombination rate are the major factors responsible for the lower laser power, which can be improved by introducing a barrier for electrons located just above the quantum well (QW). This barrier, which is also often called a decomposition preventing layer, will stop these electrons from leaving the p-type layer,[9] which should stop InGaN QW decay if it is overgrown with the other p-type material. In later studies, this barrier was called an electron blocking layer, and it became essential for all optoelectronic devices based on metal–nitride semiconductors.[10] P-doped metal nitrides (for example by Mg) region and mixed metal nitride with high Al content might have lower hole injection efficiency in the active region, which negatively affects LD performance. To solve the problems associated with this issue, several solutions were proposed for DUV LDs. Most of them focused on the EBL layer design, such as AlGaN/GaN EBL with a superlattice structure[11] and simple AlGaN-based EBL[12] both with gradual Al content transition, quaternary AlInGaN-based EBL,[13,14] multiple quantum barrier AlInGaN/GaN EBL[15] as well as step-graded AlGaN EBL.[16] To improve the hole injection efficiency, some scientists reported the implementation of AlGaN/AlGaN superlattice EBL as a mean of energy band modification for faster hole injection into the active region.[17] Other solutions to reduce valence band barrier also include the using of gradient EBLs[18] and inverted-V-shaped gradient Al-based EBLs.[19]

While the previous research on EBL enhancement was important and encouraging, further investigations are still required to find an effective and straightforward solution

*Project supported by the Special Project for Inter-government Collaboration of State Key Research and Development Program, China (Grant No. 2016YFE0118400), the Key Project of Science and Technology of Henan Province, China (Grant No. 172102410062), and the National Natural Science Foundation of China and Henan Provincial Joint Fund Key Project (Grant No. U1604263).

†Corresponding author. E-mail: iefwang@zzu.edu.cn
‡Corresponding author. E-mail: ieyhliu@zzu.edu.cn

© 2020 Chinese Physical Society and IOP Publishing Ltd

to suppress electrons' overflow and enhance hole injection simultaneously.[6] Step-like and Al-composition graded quantum wells have been the reported to provide the better modulation of carrier distribution in the quantum wells to increase the overlap between electron and hole wavefunction, which contributes to more efficient recombination of electrons and holes.[6] Compared with the conventional QB structures, the step-like QB is promising to demonstrate a better radiative recombination rate and larger maximum output power. Therefore, in this work the carrier concentration and radiative recombination rate of different EBLs with step-like QB are compared with each other. The output characteristics of LDs with different EBL structures are also investigated.

2. Simulation model

Deep ultraviolet $Al_{0.56}Ga_{0.44}N$/ $Al_xGa_{1-x}N$ single quantum well (SQW) LD structures used in this work are schematically shown in Fig. 1. The initial structure containing AlGaN EBL was a modified laser structure.[20] It consists of two 3-nm-thick $Al_{0.90}Ga_{0.10}N$ layers, two 3-nm-thick $Al_{0.94}Ga_{0.06}N$ layers, and one 3-nm-thick $Al_{0.98}Ga_{0.02}N$ layer. Based on this EBL, a step-like QB was adjusted to this LD. The LD was composed of one 500-nm-thick n-$Al_{0.78}Ga_{0.22}N$ cladding layer, one 100-nm-thick n-$A_{l0.75}Ga_{0.25}N$ waveguide layer, one 3-nm-thick $Al_{0.56}Ga_{0.44}N$ QW layer, two 4-nm-thick $Al_xGa_{1-x}N$ QB layers (which, in turn, included one 1-nm-thick $Al_{0.72}Ga_{0.28}N$, one 1-nm-thick $Al_{0.69}Ga_{0.31}N$ and one 2-nm-thick $Al_{0.66}Ga_{0.34}N$ layers), one 15-nm-thick undoped AlGaN EBL, one 150-nm-thick p-$Al_{0.75}Ga_{0.25}N$ waveguide layer, and one 500-nm-thick p-$Al_{0.78}Ga_{0.22}N$ cladding layer. During simulations, the cavity length and the laser width were 500 μm and 4 μm, respectively. The mirror reflectivity and background loss were set to be 0.05 and 2400, respectively. Si and Mg were used as materials for n-type and p-type doping, respectively. Al and Au were added to the n-type and p-type contact layers, respectively. The laser structure was designed by using the Simulastip. Laser performance was analyzed using Crosslight software. All simulations relevant to DUV LDs were performed for room temperature.

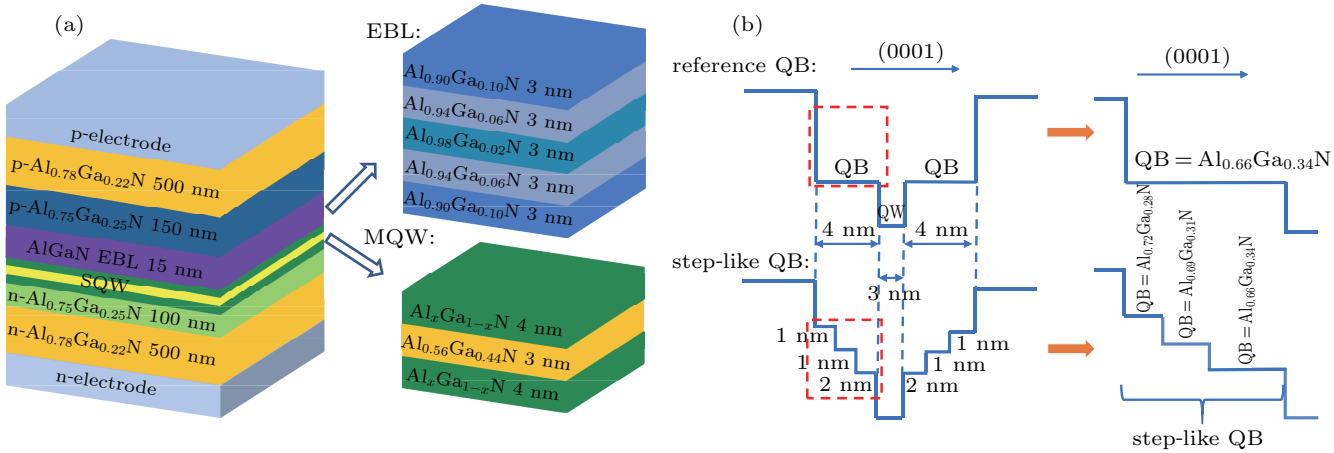


Fig. 1. (a) Schematic diagram of ultraviolet laser diode epitaxial layer structure. (b) Cross-sectional and Al composition profiles of reference QB and step-like QB with different amounts of Al content based on DUV LD emitting at ∼ 270 nm. Reference QB has no grading.

3. Results and discussion

The profile of electron concentration distribution and hole concentration distribution within SQWs are shown in Figs. 2(a) and 2(b), respectively. It can be seen that both electron and hole concentration of the LD using step-like QB are higher than those of LD using reference QB.[21] Figure 2(c) shows the radiative recombination of AlGaN SQW LDs with reference QB and step-like QB as a function of their corresponding vertical position. Holes and electrons tend to shift the QW, thus resulting in an enhanced electron–hole wavefunction overlap. The step-like QB causes the higher radiative recombination in the quantum well and leads the electrons and holes to greatly accumulate in the quantum well compared with the reference QB. The reference QB and step-like QB each reach their maximum in the middle of their corresponding quantum well, specifically ∼ 2.4 and 3.7 respectively. This, in turn, leads to a higher radiative recombination rate, and, as a result, to better output power. The light output for DUV LDs containing either reference-like QB or step-like QB is shown in Fig. 2(d). The AlGaN SQW with step-like QB structure shows that the output power and slope efficiency are higher than those of the LD containing reference QB. When the reference QB is replaced by the step-like QB, the output power significantly improves because of the enhanced radiative recombination rate. The maximum output power of the step-like QB and reference QB are 85.69 W and 65.92 W, respectively. When reference QB reaches its maximum value, the output power of step-like QB becomes 66.86 W under the same current. The slope efficiency of step-like QB is increased by ∼ 1.5% compared with that of the reference QB. Threshold voltage and current as well as resistance slightly increase (see Fig. 2(d)), possibly owing to the increase of Al in step-like QB.

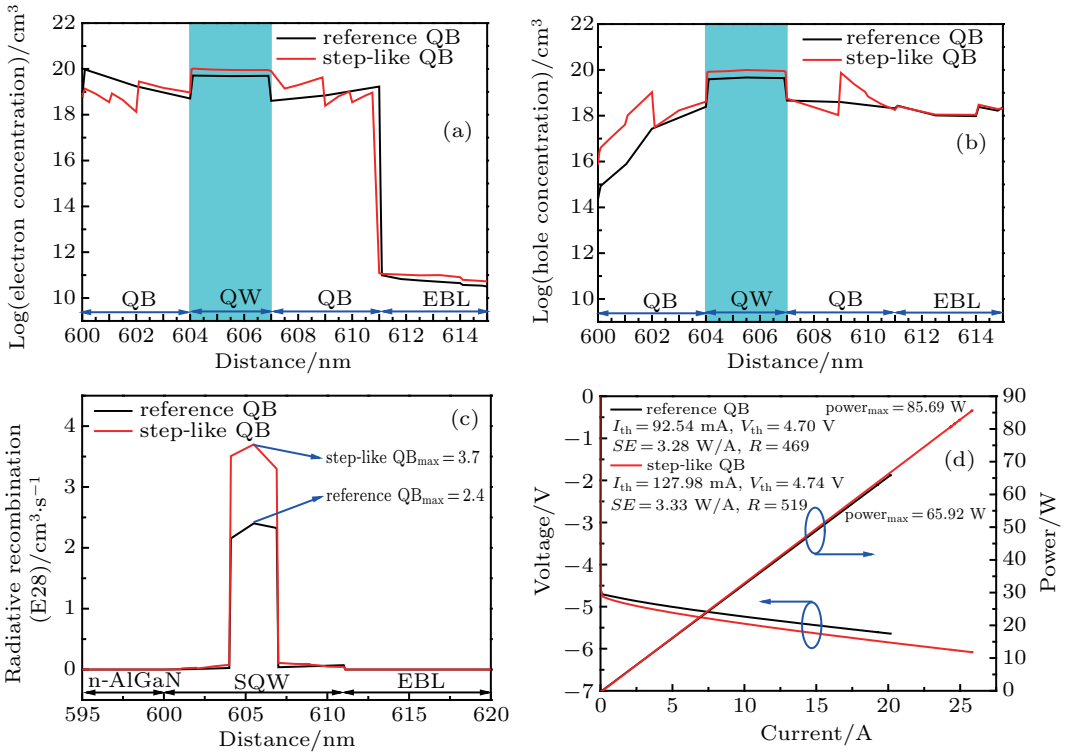


Fig. 2. (a) Electron concentration distribution, (b) hole concentration distribution, (c) radiative recombination rate distribution near SQW region, and (d) light output characteristics as a function of the injection current of DUV LD with reference QB and step-like QB.

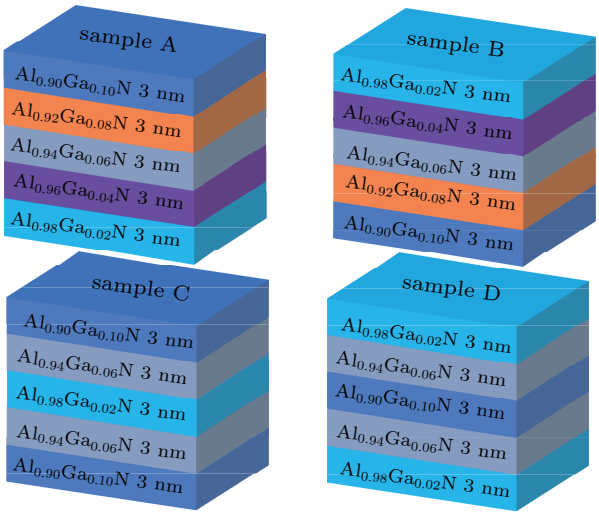


Fig. 3. Schematic diagram of the four EBLs with different Al-composition graded structures.

Compared with the LDs containing reference QB, radiative recombination rate, output power, and slope efficiency of LDs containing step-like QBs are significantly enhanced. The electron blocking layer is an important part of the laser structure. Therefore, in the next set of experiments the step-like QB is used to study the photoelectric properties of LDs containing four different EBLs, the structures of which are shown in Fig. 3. First, the optical confinement factor for LDs based on samples A, B, C, and D are simulated. Figures 4(a)–4(d) show the refractive index profiles (right axis) and optical field distributions (left axis) for the fundamental waveguide mode of samples A–D, respectively. The optical confinement factors for the four samples are similar to each other. However, sample C shows slightly higher value (equal to ~ 0.701). Larger optical confinement factor is equivalent to a higher photoelectric conversion efficiency. It can directly affect the output efficiency of the LDs. The slight improvement of the optical confinement probably occurs because of the larger refractive index between the active region and the electron blocking layer. The energy band diagram near the MQWs is calculated by self-consistently considering both spontaneous and piezoelectric polarization fields included in the Crosslight software.

Figure 5 shows the band diagram of samples A,[22] B,[23] C,[20] and D[24] near the electron blocking layer. The grading significantly affects the slopes of the EBL conduction and valence bands. The electron effective potential height will increase when AlGaN with high Al content is placed near the active region. The conduction band for the samples A and D are the highest, which leads the electrons to be effectively confined in a more active region. On the contrary, the hole effective potential height of the EBL will decrease which means the better ability to promote holes passing through the EBL to the active region. Additionally, The EBL grading can significantly modify the EBL conduction and valence band offset (E_c and E_v, respectively) since the last QB is located near the EBL. The E_c value for the electron blocking in samples A, B, C, and D are 453, 311, 310, and 453 meV, respectively. The E_v values, which are typically related to the hole diffusion, are

75, 81, 83, and 75 meV for the samples A, B, C, and D, respectively. Samples A and D demonstrate similar E_c and E_v values mostly because their active regions are the same. Thus, it will be easy to predict the same electron overflow and the same hole concentration in the SQW for these two samples. Compared with samples A and D, the effective potential height for the electron of the sample C is low (310 meV), which is beneficial for the increase of the electron leakage and the hole consumption in the p-type layer. This hole injection efficiency is expected to be weaker.

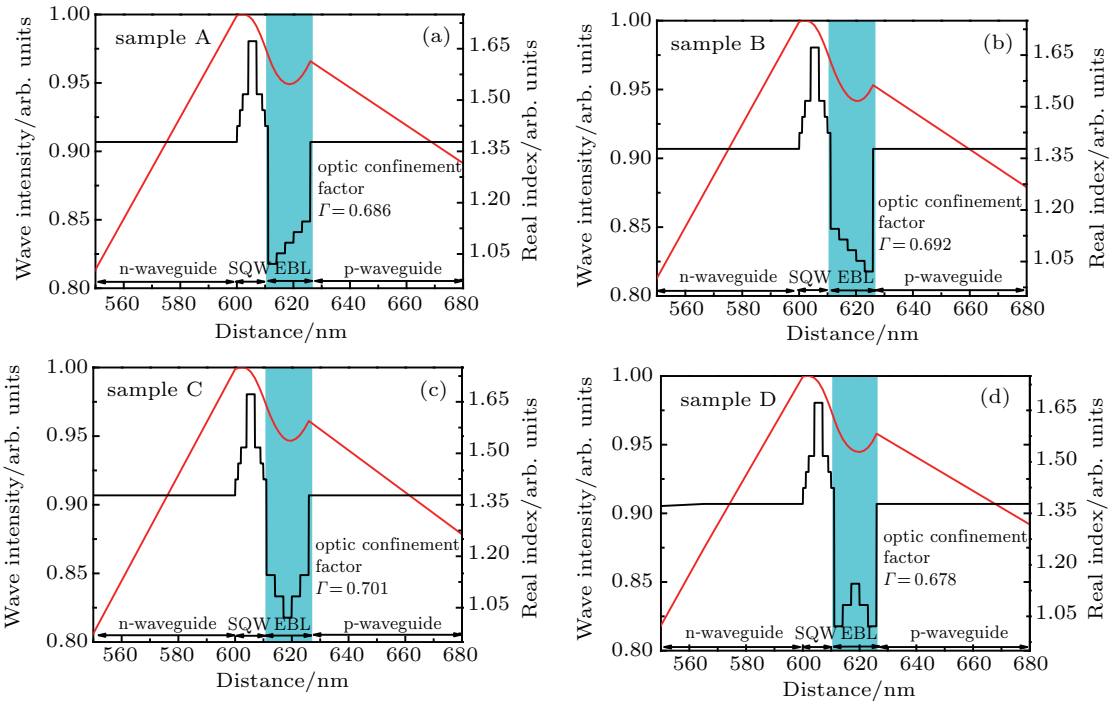


Fig. 4. Optical field distribution (left axis), and refractive index profile (right axis) for LDs with different EBLs: samples (a) A, (b) B, (c) C, and (d) D.

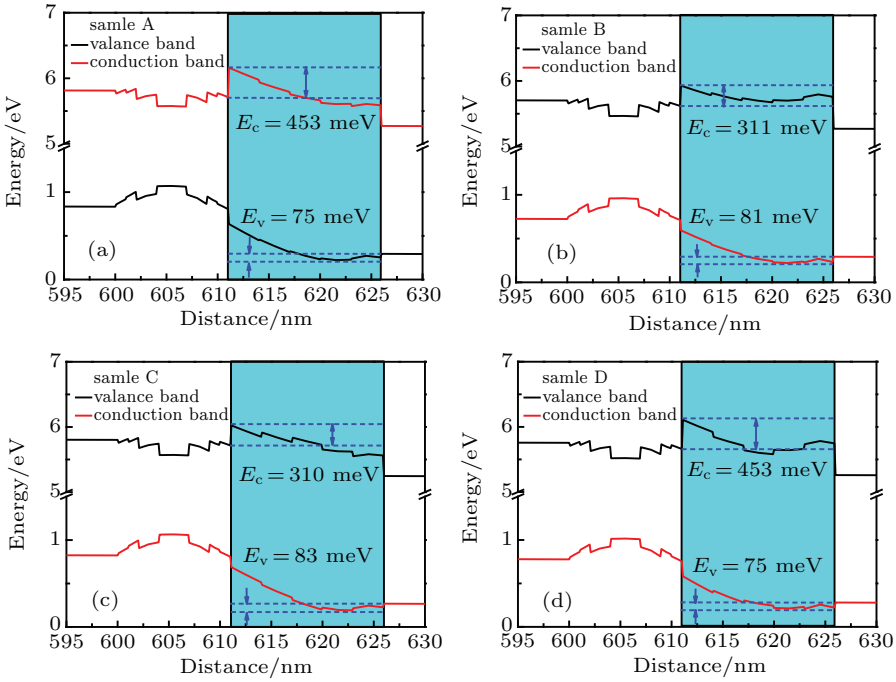


Fig. 5. Band diagrams of active regions and EBLs of samples (a) A, (b) B, (c) C, and (d) D, with cyan area indicating the EBLs with conduction and valence band offsets E_c and E_v.

Electron current, injected from the n-type layers into the active region and then overflown into the p-type layers, is viewed as an electron leakage current (see Fig. 6(a)). The electron leakage current is inversely proportional to the electron barrier height (see Fig. 5). Thus, samples A and D possess lower leakage currents because of their higher electron potential heights. Electron leakage value for samples A, B, C, and D are 13.31, 15.34, 15.56, and 13.28, respectively. These values

indicate that samples A and D can substantially facilitate electron transport and injection. Similarly, the holes, which diffuse from the p-type layers into the active region and then overflow into the n-type layers, are viewed as the hole diffusion. Corresponding values for our four samples differ from each other only slightly. Sample A has the highest hole diffusion coefficient. Radiative recombination rate within the active regions of samples A and D are higher than that of samples B and C (see Fig. 6(b)). The radiative recombination rate of sample D is 0.04 higher than of that of sample A. Sample D has the highest radiative recombination rate in all the four samples, which is confirmed by its spontaneous emission rate.

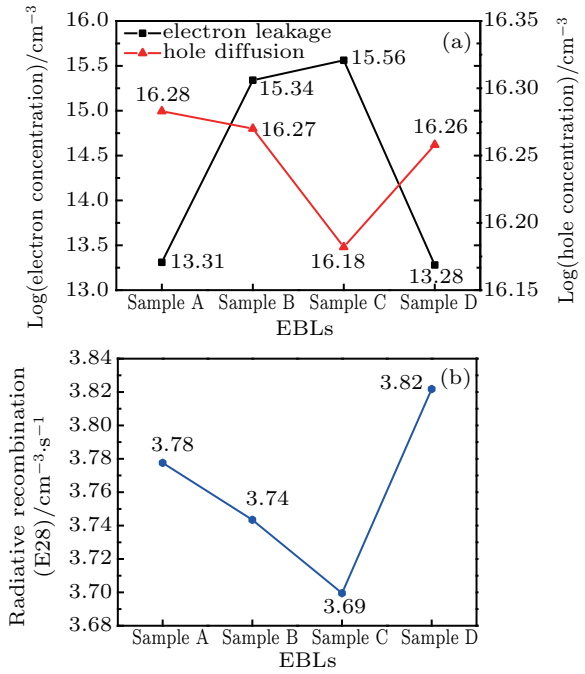


Fig. 6. (a) Logarithmic electron concentration and logarithmic hole concentration, and (b) peak radiative recombination rate in the middle QW of active region of samples A, B, C, and D.

Table 1 shows the output characteristics of LDs fabricated by using samples A–D. LDs containing samples B and C each show a lower threshold current than LDs containing samples A and D because of higher electron leakage. The threshold current value for samples A, B, C, and D are 132.1, 128.4, 127.8, and 133.9 mA, respectively. Because samples A and D possess the higher radiative recombination rates they also show higher slope efficiencies. Sample A exhibits the best performance in terms of its maximum output power, specifically, ∼ 94.36 W.

Table 1. Output characters of LDs for samples A, B, C, and D.

Types	I_{th}/mA	V_{th}/V	SE/(W/A)	R/mΩ	Power$_{max}$/W
Sample A	132.1	4.589	3.332	54.0	94.36
Sample B	128.4	4.591	3.331	50.3	93.93
Sample C	127.8	4.738	3.331	52.3	85.70
Sample D	133.9	4.591	3.332	54.0	89.99

4. Conclusions

Performance characteristics of the deep ultraviolet AlGaN/AlGaN SQW LD emitting at 270 nm are simulated and optimized by using Crosslight software. To improve the carrier concentration and radiative recombination rate of deep ultraviolet AlGaN/AlGaN SQW LDs, different structures of quantum barrier and AlGaN EBL are simulated. The simulation results show that the implementation of a step-like QB improves the radiative recombination rate and maximum output power. For LDs with EBLs containing different amounts of Al content, the placement of AlGaN with high Al content close to the active region causes higher effective potential height for electron and lowers electron current leakage, which enhances radiative recombination.

References

[1] Wunderer T, Chua C L, Yang Z, Northrup J E, Johnson N M, Garrett G A, Shen H and Wraback M 2011 *Appl. Phys. Express* **4** 092101
[2] Abe S, Sato S, Ito E, Tsukuda M, Tomiyama M and Ohno E 2002 *Jpn. J. Appl. Phys.* **41** 1704
[3] Yoshida H, Yamashita Y, Kuwabara M and Kan H 2008 *Appl. Phys. Lett.* **93** 241106
[4] Yang W, Li D, Liu N, Chen Z, Wang L, Liu L, Li L, Wan C, Chen W, Hu X and Du W 2012 *Appl. Phys. Lett.* **100** 031105
[5] Bojarska A, Goss J, Stanczyk S, Makarowa I, Schiavon D, Czernecki R, Suski T and Perlin P 2018 *Superlattices Microstruct.* **116** 114
[6] Ren Z, Lu Y, Yao H, Sun H, Liao C, Dai J, Chen C, Ryou J, Yan J, Wang J, Li J and Li X 2019 *IEEE Photon. J.* **11** 8200511
[7] Shervin S, Oh S K, Park H J, Lee K, Asadirad M, Kim S, Kim J, Pouladi S, Lee S and Li X 2018 *J. Phys. D: Appl. Phys.* **51** 105105
[8] Kim M, Schubert M F, Dai Q, Kim J K, Schubert E F, Piprek J and Park Y 2007 *Appl. Phys. Lett.* **91** 183507
[9] Nakamura S, Senoh M, Nagahama S, Iwasa N, Yamada T, Matsushita T, Sugimoto Y and Kiyoku H 1996 *Appl. Phys. Lett.* **69** 4056
[10] Piprek J and Nakamura S 2002 *IEEE Lester Eastman Conference on High Performance Devices*, August 6–8, 2005, Newark, Delaware, p. 254
[11] Zhang Y Y and Yin Y A 2011 *Appl. Phys. Lett.* **99** 221103
[12] Alahyarizadeh G, Hassan Z, Thahab S M, Yam F K and Ghazai A J 2013 *Optik* **124** 6765
[13] Ghazai A J, Thahab S M, Hassan H A and Hassan Z 2011 *Opt. Express* **19** 9245
[14] Lee S, Cho S Y, Ryu H Y, Son J K, Paek H S, Sakong T, Jang T, Choi K K, Ha K H, Ha M H, Yang M H, Nam O H and Park Y 2006 *Appl. Phys. Lett.* **88** 111101
[15] Zhang N, Liu Z, Wei T, Zhang L, Wei X, Wang X, Lu H, Li J and Wang J 2012 *Appl. Phys. Lett.* **100** 053504
[16] Zhang Y, Kao T, Liu J, Lochner Z, Kim S, Ryou J, Dupuis R D and Shen S 2011 *J. Appl. Phys.* **109** 083115
[17] Yin Y A, Wang N, Li S, Zhang Y and Fan G 2015 *Appl. Phys. A* **119** 41
[18] Zhang Y, Yu L, Li K, Pi H, Diao J, Wang X, Shen Y, Zhang C, Hu W, Song W and Li S 2015 *Superlattices Microstruct.* **82** 151
[19] Fan X, Sun H, Li X, Sun H, Zhang C, Zhang Z and Guo Z 2015 *Superlattices Microstruct.* **88** 467
[20] Liu C, Ren Z, Chen X, Zhao B, Wang X and Li S 2014 *IEEE Photon. Technol. Lett.* **26** 1368
[21] Lu L, Zhang Y, Xu F J, Ding G G and Liu Y H 2018 *Superlattices Microstruct.* **118** 55
[22] Yang W, Li D, He J and Hu X 2013 *Phys. Status Solidi C* **10** 346
[23] Satter M M, Lochner Z, Member S, Kao T, Liu Y, Li X, Shen S, Dupuis R D and Yoder P D 2014 *IEEE J. Quantum Electron.* **50** 166
[24] Wang Y, Niass M I, Wang F and Liu Y 2019 *Chin. Phys. Lett.* **36** 057301